JOURNAL OF SOLID STATE CHEMISTRY 27, 397–405 (1979)

The Ionic Conductivity of PbFCl

A. F. HALFF AND J. SCHOONMAN

Physical Laboratory, Solid State Chemistry Department, State University, Sorbonnelaan 4, Utrecht, The Netherlands

Received March 9, 1978; in final form July 3, 1978

Ionic conductivity results on PbFCl both parallel and perpendicular to the crystallographic c axis are reported. In conjunction with transference numbers, aliovalent dopant effects, ^{19}F NMR and structural considerations mechanisms governing the ionic conductivity in PbFCl are proposed. Experimental ΔH_m values are related with the defect jumps involved. The formation enthalpy for a set of Schottky defects in PbFCl is presented.

1. Introduction

In previous papers we have reported on electrical (*1–3*) and photo-electrical (*4*) properties of ternary lead fluorohalides. In spite of the fact that the electrical conductivity of $PbCl_2$ (*5*) and of β-PbF_2 (*6*) is presently well understood, little is known about the transport mechanism governing the ionic conductivity of PbFCl. It has been proposed that intrinsic defects are thermally generated according to a Schottky mechanism (*1*), and that both anions are mobile in PbFCl (*2, 3*).

Recently, we have reported on the influence of deviations from the ideal composition of $PbFX$ ($X = Cl$, Br) on the ionic conductivity (*7*). It has been shown that the extrinsic conductivities of melt-grown undoped crystals are governed by the extent of formation of solid solutions of composition $PbF_{1-x}X_{1+x}$ and $PbF_{1+x}X_{1-x}$, and by oxygen impurities. It seems possible from the conductivity data to distinguish between crystals wherein oxygen impurities predominate over the deviation from molecularity, and crystals wherein the reversed situation holds.

PbFCl has a tetragonal layer structure (*8, 9*). The unit cell consists of plane sheets perpendicular to the crystallographic c axis, with layer sequence F Pb Cl Cl Pb F. It has been established that this structure favors anisotropic conductivity (*1, 7*).

The anisotropy can be used to obtain additional information about the conduction mechanism (*10*). In order to characterize this mechanism for PbFCl, the ionic conductivity of undoped crystals has been measured parallel and perpendicular to the crystallographic c axis, and of crystals doped with aliovalent metal halides parallel to the c axis. In addition, transference numbers of ions, and ^{19}F dipolar motional narrowing have been determined for polycrystalline PbFCl.

2. Experimental

In this study crystals were employed which were grown from equimolar melts of PbF_2 and $PbCl_2$. The procedure has been published elsewhere (*1, 7*). Doping with thallium was done by adding thallium(I) chloride (BDH) before zone melting. Bismuth (Merck) was introduced by placing a small

0022-4596/79/030399-09$02.00/0

amount of the metal at the beginning of the tube. Doped crystals were often more or less opaque. Only Bi-doped crystals had suitable dimensions to measure the conductivity perpendicular to the c axis also.

For transference number measurements and in several cases for a.c. conductivity studies pellets were used. The diameter of the compacts was 1.29 cm while thicknesses varied from 0.08 to 0.15 cm. Before electrolysis the pellets were sintered for about 60 hr at about 625°K in a purified nitrogen ambient to improve their density.

A preliminary nuclear magnetic resonance study has been made of ionic motion in polycrystalline PbFCl. The fluorine NMR signal was observed using a crossed-coil Varian 4200 spectrometer, details of which have been published before (*11*).

The experimental set-up for the a.c. conductivity measurements has been published elsewhere (*7*). In addition admittance parameters of PbFCl ($\perp$ and $\parallel$ c axis) between ionically blocking platinum electrodes were recorded in the range 10^{-2} Hz–10 kHz using a Solartron Frequency Response Analyzer (1170). Complex-plane analysis of the frequency dispersion revealed the low-frequency intercept to be at the origin indicating negligible electronic conductivity.

Transference numbers were measured by the method of Tubandt and co-workers (*12*) and of Bénière (*13, 14*). The data were obtained with the cells

$$\oplus C|Y_1|Y_2|Y_3|X_1|X_2|X_3|Y_4|Y_5|Y_6|C\ominus \qquad (I)$$

and

$$\oplus C|X_1|X_2|X_3|Ag|AgI|C\ominus \qquad (II)$$

where X_i denotes a PbFCl pellet and Y_i a $PbCl_2$ ($t_{Cl} = 1$) (*5*) pellet. In several cases pellets Y_1 to Y_3 were replaced by β-PbF_2 pellets ($t_F = 1$) (*6*). Currents of about 0.3 mA were provided by a constant-current source, and were measured as a function of time with an autoranging picoammeter (Keithley 445) coupled to a Solartron data transfer unit and a tape punch. The weight decrease of the silver electrode and the weight increase of the AgI pellets in cell II agreed very well with the recorded charge flow, indicating that silver was deposited from the cathode as dendrites in AgI, and that lead was not deposited on the silver electrode but as dendrites in PbFCl (*3*). The right-hand part of electrolysis cell II can, therefore, be used as a coulometer. Reliable results could be obtained when the charge passed through the cell exceeded 10 C.

3. Results

3.1. Ionic Conductivity Measurements

The temperature dependence of the ionic conductivity of undoped PbFCl crystals along and perpendicular to the crystallographic c axis is presented in Fig. 1. In most cases melt-grown PbFCl crystals exhibit conductivity anomalies at temperatures close to the PbFCl–$PbCl_2$ eutectic, i.e. at about 730°K, indicating excess $PbCl_2$ (*7*). It has been demonstrated (*7*) that the composition of crystals grown from equimolar mixtures of the binary constituents can be close to the ideal one. The data gathered in Fig. 1 refer to undoped crystals with almost ideal composition.

Results of undoped PbFCl, and crystals doped with thallium and bismuth measured parallel to the c axis are gathered in Fig. 2. The data for Bi-doped PbFCl measured perpendicular to the c axis have been included as well. The steep increase of the conductivity of all these samples for temperatures greater than about 675°K closely resembles the increase of the conductivity of $PbCl_2$-rich PbFCl crystals in the temperature region close to the PbFCl–$PbCl_2$ eutectic. At low and moderate temperatures the conductivity increases with respect to the conductivity of undoped PbFCl by incorporation of monovalent impurities, and decreases upon doping with

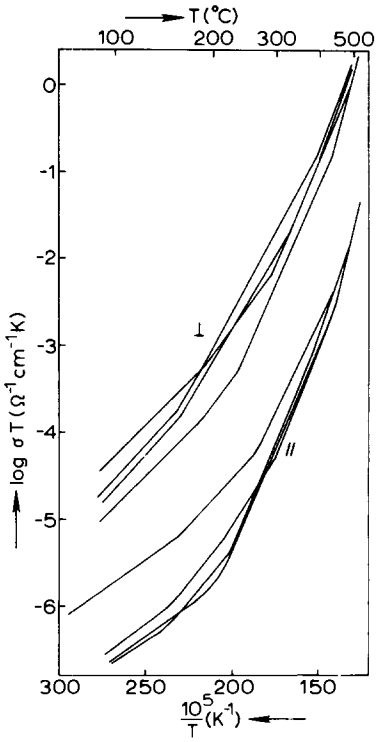

FIG. 1. The ionic conductivity of undoped PbFCl crystals measured parallel and perpendicular to the c axis.

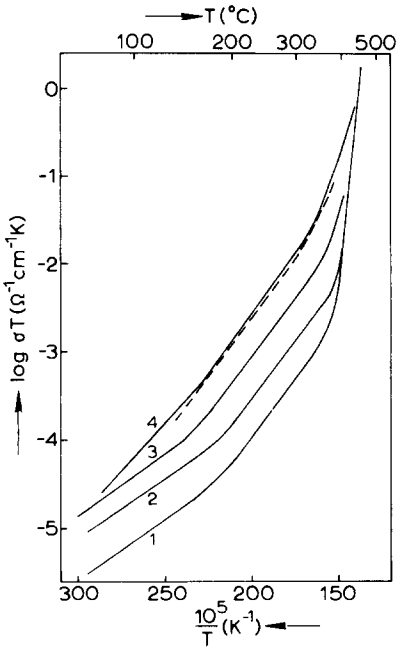

FIG. 2. The ionic conductivity ($\parallel c$ axis) of PbFCl crystals doped with thallium or bismuth, and their undoped starting material. (1) PbFCl:Bi (17 ppm); (2) undoped; (3) PbFCl:TlCl (64 ppm); (4) PbFCl:TlCl (244 ppm). The dotted line represents data for Bi-doped PbFCl ($\perp c$ axis).

trivalent impurities. The experimental data as gathered in Figs. 1 and 2 have been subjected to graphical fitting to a sum of three exponential functions of the type $\sigma = \sigma_i^0/T \exp(-\Delta H_i/kT)$. The values for ΔH_i, ranging from low to high temperatures (sequence 1–3), are gathered in Table I. For comparison ΔH_i values of polycrystalline (p.c.) PbFCl have been included in Table I. The PbFCl (p.c.) data refer to material that has been obtained by grinding undoped PbFCl crystals of which data are shown in Fig. 2. Similar results were obtained for PbFCl:Bi (p.c.). For the magnitude of the conductivity it was found that σ(PbFCl, p.c.) $>\sigma$(PbFCl:Bi, p.c.), while σ(p.c.) $>\sigma(\parallel)$. A comparison between the data presented in Fig. 1 (A), Ref. 7 (B), and Fig. 2 (C) reveals for the undoped PbFCl crystals

$$\sigma(\parallel; \text{A, B}) \ll \sigma(\parallel; \text{C}) < \sigma(\perp; A, B).$$

From the conductivity data presented in Fig. 2 conductivity isotherms, i.e. σ versus dopant concentration were constructed. From the linearity of these isotherms (Fig. 3) it may be concluded that the nominally pure and doped crystals have the same mobile defect in the temperature region involved. From these isotherms, the temperature dependence of its mobility can be calculated to be

$$\mu T = 1.1 \times 10^3 \times \exp(-0.6\ \text{eV}/kT)\ \text{cm}^2\ \text{K}\ \text{V}^{-1}\ \text{s}^{-1}. \quad (1)$$

3.2. Transference Numbers

In cell I the guard electrodes $PbCl_2$ are pure anionic conductors. For PbFCl the absence of an electronic contribution to the conductivity implies $t_{Pb} + t_F + t_{Cl} = 1$. In order

TABLE I

CONDUCTIVITY ACTIVATION ENTHALPIES FOR PbFCl CRYSTALS

	ΔH_1 (eV)	ΔH_2 (eV)	ΔH_3 (eV)	Reference
PbFCl ($\parallel c$ axis)	0.29 ± 0.03	0.84 ± 0.06	1.7 ± 0.1	This work, Fig. 1
PbFCl ($\parallel c$ axis)	0.28	0.70	3.2	This work, Fig. 2
PbFCl ($\parallel c$ axis)	0.34	0.81[a]	1.8[a]	7
PbFCl:Tl ($\parallel c$ axis)				
244 ppm	0.40	0.63	—	This work, Fig. 2
64 ppm	0.25	0.68	—	This work, Fig. 2
PbFCl:Bi ($\parallel c$ axis)				
17 ppm	0.27	0.69	3.2	This work, Fig. 2
PbFCl ($\perp c$ axis)	0.34 ± 0.03	0.66 ± 0.06	1.55 ± 0.16	This work, Fig. 1
PbFCl:Bi ($\perp c$ axis)	—	0.53	—	This work, Fig. 2
PbFCl (p.c.)	0.26	0.71	—	This work

[a] Inferred from curve 3 in Fig. 1, Ref. 7.

to derive the transference number equation, we consider pellets Y_3 and X_1 as a unit. A Faraday equivalent of chloride leaves Y_3 for Y_2 for each coulomb of charge passed. The charge will be transported at the other interface between pellets X_1 and X_2 by Pb^{2+}, F^- and Cl^- ions, so that we expect less than a Faraday equivalent of lead to enter X_2 from X_1 and a supplementary amount of chloride and fluoride to leave X_2 for X_1. For the change of weight of pellets Y_3 and X_1 together one obtains

$$\Delta w(Y_3 - X_1) = (t_F A_F + t_{Cl} A_{Cl} - A_{Cl} - \tfrac{1}{2} t_{Pb} A_{Pb}) Q/F \qquad (2)$$

where A_i denotes atomic weight, the charge Q is in coulombs, and the weight change is in grams. F is Faraday's constant. In cell I arrangements pellets $Y_3 - X_1$ should undergo a weight decrease while pellets $X_3 - Y_4$ should experience a corresponding increase, and pellets Y_2, X_2 and Y_5 should not change at all.

Since the sum of the transference numbers is unity we can rewrite Eq. (2) as

$$\Delta w(Y_3 - X_1) = [t_F(A_F - A_{Cl}) - t_{Pb}(\tfrac{1}{2} A_{Pb} + A_{Cl})] Q/F. \qquad (3)$$

After passage of an amount of charge larger than 10 C at 323°K the weight changes $\Delta w(Y_3 - X_1)$ and $\Delta w(X_3 - Y_4)$ were not beyond the experimental error (0.3 mg). In the case that PbFCl was electrolyzed at 452°K between β-PbF_2 and $PbCl_2$ pellets $\Delta w(X_3 - Y_4)$ was also practically zero, while $\Delta w(Y_3 - X_1)$ showed an increase. All these results indicate $t_{Pb} \ll t_F < t_{Cl}$. For the determination of the individual transference numbers cell II was employed. The weight

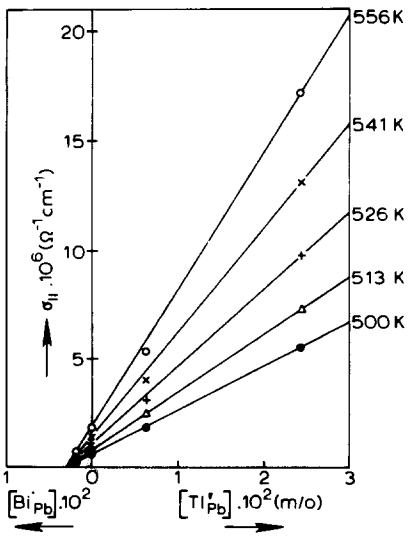

FIG. 3. Conductivity isotherms as constructed from the data presented in Fig. 2.

decrease of pellet X_1 can be represented by

$$\Delta w(X_1) = -\tfrac{1}{2} t_{Pb} A_{Pb} Q/F \qquad (4)$$

under the condition that t_F of an equivalent of fluoride and t_{Cl} of an equivalent of chloride escape at the anode side as F_2 and Cl_2, respectively. The weight change of the silver electrode indicated that lead is not deposited on this electrode. Therefore, $\Delta w(X_3)$ can be represented by

$$\Delta w(X_3) = (\tfrac{1}{2} t_{Pb} A_{Pb} - t_F A_F - t_{Cl} A_{Cl}) Q/F. \qquad (5)$$

From the weight decrease of pellet X_1 we obtained for undoped PbFCl in the region 497–551°K for t_{Pb} 0.01–0.03, for PbFCl:Tl at 526°K $t_{Pb} = 0.03$ and for PbFCl:Bi at 548°K $t_{Pb} = 0.03$. It should be noted, however, that for amounts of passed charge in the range 10–25 C the decrease of pellet X_1 did not exceed 1×10^{-3} g. In view of the experimental error it may therefore be assumed that lead ions are immobile in PbFCl. Electrolysis of one pellet in cell II should then result in a weight decrease of $-(t_F A_F + t_{Cl} A_{Cl}) Q/F$. Under the condition $t_F + t_{Cl} = 1$ the data obtained with cell I lead to $t_{Cl} = 1$ in the region 323 to 452°K. In Table II we have gathered the experimentally determined transference numbers. The data are consistent with previously reported values for t_{Cl} (*3*) in undoped and doped material, and reveal that in polycrystalline PbFCl chloride ion conduction predominates at low temperatures, and that at high temperatures fluoride ion conduction predominates.

TABLE II

TRANSFERENCE NUMBERS OF THE IONS IN UNDOPED AND DOPED POLYCRYSTALLINE PbFCl (CELL II)

Material	T (K)	t_{Cl} ($= 1 - t_F$)	Number of pellets
PbFCl	497	0.82	3
PbFCl	530	0.62	1
PbFCl	538	0.45	1
PbFCl	545	0.62	1
PbFCl	551	0.35	3
PbFCl:Tl	526	0.89	3

3.3. ^{19}F Nuclear Magnetic Resonance

The peak-to-peak separation of the derivative absorption mode of the ^{19}F resonance varied with temperature as presented in Fig. 4. Motional narrowing of the resonant species in PbFCl (for σ: see Fig. 2) occurred between 300 and about 380°K. The signal became half-narrowed at 328°K; above that temperature the spectra appeared to be Lorentzian. The rigid lattice linewidth was about 5 G. The dipolar motional narrowing data were analyzed assuming a linear relationship between the transverse relaxation time T_2 and the jump frequency for thermally activated motion in a random walk model. The usual expression for the temperature dependence of the jump frequency is

$$\nu = \nu_0 \exp(\Delta S_m/k) \exp(-\Delta H_m/kT). \qquad (6)$$

With the dipolar linewidth dH_d inversely proportional to T_2, this leads to (*15*)

$$dH_d = dH - dH_r = C \exp(\Delta H_m/kT). \qquad (7)$$

Here C is a constant, and ΔH_m the activation enthalpy of migration. The dipolar contribution to the linewidth dH_d is found from the experimental linewidth dH by subtracting

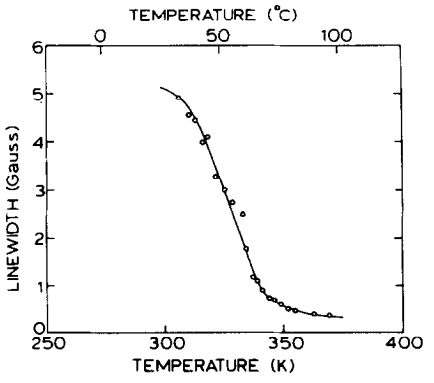

FIG. 4. The temperature dependence of the linewidth of the fluorine magnetic resonance absorption in polycrystalline PbFCl.

the temperature-independent residual linewidth dH_r (0.292 G). For ΔH_m a value of 0.76 ± 0.05 eV resulted. This value is in agreement with the conductivity activation enthalpy ΔH_2 (0.71 eV) for undoped polycrystalline PbFCl (see Table I).

4. Discussion

The transference numbers of the ions in undoped and doped polycrystalline PbFCl clearly substantiate that the material is an anionic conductor. The change-over from chloride ion to fluoride ion conduction in polycrystalline PbFCl has been reported (*3*) to occur between 520 and 560°K. The data in Table II indicate that the region where mixed anionic conduction prevails may be extended to lower temperatures. In regard to the layered tetragonal structure of PbFCl which evidently leads to anisotropic conductivity, the mechanism of conduction along and perpendicular to the c axis will be different, and thus the temperature regions wherein mixed anionic conduction will prevail. That these regions are larger for single crystals can readily be seen from the data presented in Figs. 1 and 2. Moreover, d.c. conductivity in polycrystalline anisotropically conducting pellets may require appreciable migration through the grain boundaries. Such effects have even been observed in isotropically conducting polycrystals (*13*). The transference number data can thus only be used qualitatively in the interpretation of the conductivity data of single crystals.

Monovalent cationic dopants increase, and trivalent cationic impurities decrease the ionic conductivity with respect to the nominally pure material. In view of the observation that t_{Pb} is virtually zero charge compensation provided by mobile interstitial lead ions in PbFCl substitutionally doped with Tl^+ ions can be ruled out. The incorporation reaction is then

$$TlCl \rightarrow Tl'_{Pb} + V_F^{\cdot} + Cl_{Cl}^{\times}. \quad (8)$$

Bismuth has been introduced as metal before zone-refining. A melt of PbFCl exhibits a substantial dissociation into the binary constituents (*16*). Molten bismuth reacts to some extent with molten PbF_2 (*17*), and molten $PbCl_2$ (*18*) under the formation of bismuth fluoride, bismuth chloride, respectively and lead. These bismuth halides can be incorporated according to the reactions

$$BiCl_3 \rightarrow Bi_{Pb}^{\cdot} + 2V''_{Pb} + 3V_F^{\cdot} + 3Cl_{Cl}^{\times} \quad (9)$$

and

$$BiF_3 \rightarrow Bi_{Pb}^{\cdot} + 2V''_{Pb} + 3F_F^{\times} + 3V_{Cl}^{\cdot}. \quad (10)$$

Since the interstitial sites in PbFCl allow ions with a radius of 0.45 Å to occupy them, the occurrence of interstitial fluoride (1.36 Å) and interstitial chloride ions (1.81 Å) is improbable (*3*). Crystal growth has been performed at 925°K (*7*). This temperature is lower than the melting point of BiF_3 (1000°K), but much higher than the melting point of $BiCl_3$ (503°K) and even its boiling point (720°K). Evaporation losses of $BiCl_3$ during crystal growth may well have occurred leading to $[BiF_3] > [BiCl_3]$. The $BiCl_3$ and an equal amount of BiF_3 can be incorporated via

$$BiF_3 + BiCl_3 \rightarrow 2Bi_{Pb}^{\cdot} + V''_{Pb} + 3F_F^{\times} + 3Cl_{Cl}^{\times} \quad (11)$$

which means the annihilation of three sets of Schottky defects, while the remaining amount of BiF_3 will be incorporated according to reaction (10). It has been emphasized that the high-temperature data in Fig. 2 indicate that $PbCl_2$-rich material has been employed. Solid solution formation according to (*7*)

$$PbCl_2 \rightarrow Pb_{Pb}^{\times} + V''_{Pb} + 2V_F^{\cdot} + 2Cl_{Cl}^{\times} \quad (12)$$

then governs the concentration of the point defects in the nominally pure starting PbFCl. The net result of doping with Bi metal would be an enhanced concentration of V''_{Pb} and $V_{Cl}^{\cdot}$. Reaction (12) reveals, however, that annihilation of point defects through the

Schottky-mechanism can result. If α represents the concentration of dissolved $BiCl_3$, β that of BiF_3 and γ that of $PbCl_2$ then the doped crystals will contain, in addition to $Bi_{Pb}^{\cdot}$, the defects V_{Pb}'' and $V_F^{\cdot}$ if $3(\beta-\alpha)<2\gamma$. This assumption is quite reasonable in view of the actual amount of Bi present in the crystal, and the extent to which solid solution formation can occur (*7*). With respect to the undoped starting material the Bi-doped PbFCl contains lower concentrations of V_{Pb}'' and $V_F^{\cdot}$. The concentration of the fluoride ion vacancies in Tl-doped PbFCl is larger than in the starting material.

Differences in the extrinsic conductivities of nominally pure PbFCl crystals as gathered in Fig. 1 are due to deviations from the ideal composition. If the $PbCl_2$ content of the solid solution increases, $[V_{Cl}^{\cdot}]$ decreases and $[V_F^{\cdot}]$ increases (Eq. 12) and compensation of oxygen impurities by the deviation from molecularity occurs as has been discussed previously (*7*). If the concentration of $PbCl_2$ increases further even associates the type $(V_{Pb}\cdot V_F)'$ may occur with a dissociation enthalpy of ~1.0 eV. If this concentration is so large that a separate phase of $PbCl_2$ and thus premelting effects close to the $PbCl_2$–PbFCl eutectic are encountered extrinsic conductivities are much higher than for the dilute solid solutions (compare the data of nominally pure PbFCl of Fig. 2 with those of Fig. 1).

In order to arrive at a conductivity mechanism we have to consider the various jumps of each of the possible mobile defects, i.e. $V_F^{\cdot}$ and $V_{Cl}^{\cdot}$, taking the anisotropy into account. The possible defect jumps in the PbFCl structure are shown in Fig. 5. We will refer to defect jumps by using their frequency as symbol, i.e. ω_a(Cl) denotes the jump of $V_{Cl}^{\cdot}$ having frequency ω_a.

4.1. Conductivity perpendicular to the *c* axis: $\sigma_\perp$

The most probable defect jump in the fluoride ion layer perpendicular to the *c* axis

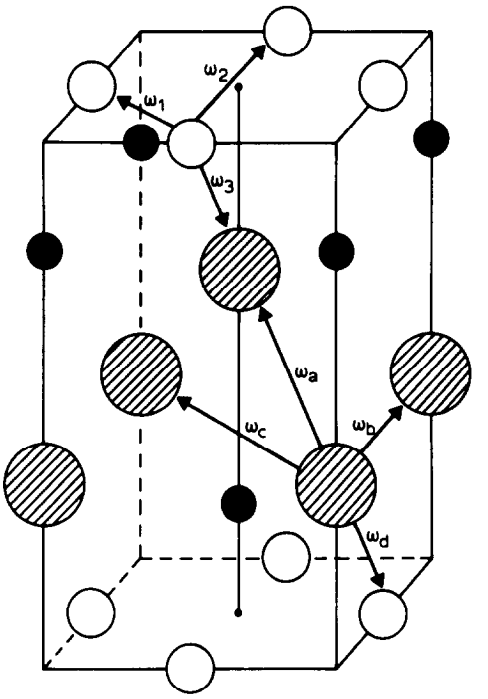

FIG. 5. Crystal structure of PbFCl and possible defect jumps. Open circles F, black circles Pb, hatched circles Cl (see text).

is $V_F^{\cdot}$ jump ω_1(F), since this jump is in the basal plane, and the F–F distance for this jump is appreciably smaller than that for jump ω_2(F), i.e. 2.89 Å against 4.09 Å.

In the chloride ion layers the jumps ω_a(Cl) and ω_b(Cl) are the most likely to occur. Jump ω_c(Cl) may be disregarded for structural reasons. The Cl–Cl distances involved in ω_a(Cl) and ω_b(Cl) are 3.62 and 4.09 Å, respectively. Jump ω_a(Cl) seems more likely to occur than jump ω_b(Cl). However, this jump contributes about equally to both $\sigma_\parallel$, while the experimental data reveal $\sigma_\perp > \sigma_\parallel$. In view of the transference numbers we therefore assign the value 0.34 eV for $\Delta H_1(\perp)$ to jump ω_b(Cl). It is quite obvious that the jump ω_1(F) only contributes to $\sigma_\perp$. The changeover from Cl to F conduction at elevated temperatures then indicates that the value 0.66 eV for $\Delta H_2(\perp)$ of undoped and 0.53 eV for $\Delta H_2(\perp)$ of Bi-doped PbFCl can be related to jump $\omega_1(F)$. The motional nar-

rowing data of polycrystalline PbFCl are probably related to this jump as well.

4.2. Conductivity parallel to the c axis: $\sigma_{\parallel}$

The decrease of the low-temperature conductivity of undoped dilute solid solutions upon increasing $PbCl_2$ content (*7*) indicates that values in the range 0.25 to 0.34 eV, ((*7*), see Table I) for $\Delta H_1(\parallel)$ should be correlated with jump ω_a(Cl). That $\Delta H_1(\parallel)$ and $\Delta H_2(\perp)$ are of the same order of magnitude indicates that the conductivity anisotropy originates primarily from a difference in the pre-exponential factor. Although this has been observed for other anisotropically conducting solids (*10*), a firm explanation is still lacking.

In addition, jump ω_d(Cl) can contribute to the conductivity parallel to the c axis of dilute solid solutions. It involves antistructure formation, and contributes to t_F in d.c. conductivity

$$V_{Cl}^{\cdot} + F_F^{\times} \rightarrow F_{Cl}^{\times} + V_F^{\cdot}, \omega_d(Cl). \quad (13)$$

We tentatively assign values in the range 0.81 to 0.84 eV for $\Delta H_2(\parallel)$ to this jump.

The data presented in Fig. 2 refer to concentrated solid solutions, wherein even $PbCl_2$ as a separate phase is present. In regard of reaction (12), and the incorporation reactions of TlCl and bismuth, V_F should be involved in jumps related with these experimental data. So far it has been argued that the concentrated solid solutions, nominally pure as well as doped, contain isolated and associated defects $V_F^{\cdot}$, V_{Pb}'' and $(V_{Pb} \cdot V_F)'$. The conductivity data in Fig. 2 do not indicate the thermal dissociation of associated defect pairs. We, therefore, must assume that jump ω_3(F) is involved. Consider the layer sequence $F_1Pb_2Cl_3Cl_4Pb_5F_6$ with isolated and associated defects in the Pb and F layers. Long-range migration starting with jump ω_3(F) can then be represented by

$$V_{F,1}^{\cdot} + Cl_{Cl,3}^{\times} \rightarrow Cl_{F,1}^{\times} + V_{Cl,3}^{\cdot}, \omega_3(F) \quad (14)$$

$$V_{Cl,3}^{\cdot} + Cl_{Cl,4}^{\times} \rightarrow Cl_{Cl,3}^{\times} + V_{Cl,4}^{\cdot}, \omega_a(Cl) \quad (15)$$

$$F_{F,6}^{\times} + V_{Cl,4}^{\cdot} \rightarrow F_{Cl,4}^{\times} + V_{F,6}^{\cdot}, \omega_d(Cl). \quad (16)$$

If via the first mechanism $Cl_{F,6}^{\times}$ were to be present then

$$Cl_{F,6}^{\times} + V_{Cl,4}^{\cdot} \rightarrow V_{F,6}^{\cdot} + Cl_{Cl,4}^{\times}$$

would complete a d.c. conduction path for Cl ($t_{Cl} = 1$) parallel to the c axis.

A similar sequence of jumps may be visualized starting from an associated defect pair, i.e.

$$(V_{Pb,2} \cdot V_{F,1})' + Cl_{Cl,3}^{\times} \rightarrow$$

$$(V_{Pb,2} \cdot V_{Cl,3})' + Cl_{F,1}^{\times}. \quad (17)$$

The next jump may cause the associate to dissociate, or, if an adjacent lead ion vacancy is present in layer (*5*)

$$(V_{Pb,2} \cdot V_{Cl,3})' + Cl_{Cl,4}^{\times} + V_{Pb,5}'' \rightarrow$$

$$V_{Pb,2}'' + Cl_{Cl,3}^{\times} + (V_{Pb,5} \cdot V_{Cl,4})'. \quad (18)$$

A next jump, involving either $F_{F,6}^{\times}$ or $Cl_{F,6}^{\times}$, would then complete a d.c. conductivity path with $t_F + t_{Cl} = 1$, or $t_{Cl} = 1$, respectively.

The values for $\Delta H_2(\parallel)$ of Fig. 2 are found in the range 0.63–0.70 eV, and are related with ω_3(F). The electrical mobility is represented by Eq. (1).

$$\omega_3(F) = 2.2 \times 10^{13} \exp(-0.6\ \text{eV}/kT)\ \text{s}^{-1}. \quad (19)$$

In order to ascribe $\Delta H_1(\parallel)$ values to ω_a(Cl), which seems the only possibility, we have to accept the presence of antistructure defects in these concentrated solid solutions. This implies that to a small extent TlCl, for example, is incorporated according to

$$TlCl \rightarrow Tl_{Pb}' + Cl_F^{\times} + V_{Cl}^{\cdot}. \quad (20)$$

As a consequence, a major fraction of the lead ion vacancies should be present as associates. The fact that $\Delta H_2(\parallel)$ for ω_3(F) is

smaller than $\Delta H_2(\|)$ for ω_d(Cl) is in line with a more open conduction path.

4.3. The formation enthalpy of Schottky defects: ΔH_f

The data in Fig. 1 can be used to evaluate the formation enthalpy. This parameter is independent of anisotropy, and can be calculated with $\Delta H_f = 3(\Delta H_3(\perp) - \Delta H_2(\perp)) = 3(\Delta H_3(\|) - \Delta H_2(\|))$. From the $\sigma_\|$ data we obtain $\Delta H_f = 2.58 \pm 0.48$ eV, while the $\sigma_\perp$ data lead to $\Delta H_f = 2.67 \pm 0.48$ eV. An estimate from reported $\sigma_\|$ data (*7*) yields for ΔH_f the value 2.97 eV (see Table I).

The sharp rise in the conductivity of the $PbCl_2$-rich concentrated solid solutions (Fig. 2) starts at temperatures lower than the $PbCl_2$–PbFCl eutectic. The large values for ΔH_3 may be related to premelting effects, i.e. the dissolution of $PbCl_2$ according to reaction (12). From the data gathered in Table I a dissolution enthalpy of about 7.5 eV can then be inferred.

Acknowledgments

We wish to acknowledge our indebtness to Professor Dr. G. Blasse for his encouraging stimulation and his valuable criticism during the preparation of the manuscript. One of the authors (J.S.) would like to thank Professor R. A. Huggins of Stanford University for providing the facilities to study motional narrowing in PbFCl.

References

1. J. SCHOONMAN, G. J. DIRKSEN, AND G. BLASSE, *J. Solid State Chem.* **7**, 245 (1973).
2. J. SCHOONMAN, A. F. HALFF, AND G. BLASSE, *Solid State Commun.* **13**, 677 (1973).
3. A. F. HALFF, J. SCHOONMAN, AND A. J. H. EIJKELENKAMP, *J. Phys.* **34**, C9-471 (1973).
4. A. F. HALFF AND J. SCHOONMAN, *Phys. Status. Solidi A* **40**, 511 (1977).
5. K. J. DE VRIES, Thesis, University of Utrecht (1965).
6. R. W. BONNE AND J. SCHOONMAN, *J. Electrochem. Soc.* **124**, 28 (1977).
7. A. F. HALFF AND J. SCHOONMAN, *Z. Phys. Chem.* N.F., in press.
8. F. A. BANNISTER AND M. H. HEY, *Mineral Mag.* **23**, 587 (1934).
9. W. NIEUWENKAMP, Thesis, University of Utrecht (1932).
10. D. S. PARK AND A. S. NOWICK, *J. Phys. Chem. Solids* **37**, 607 (1976).
11. J. SCHOONMAN, L. B. EBERT, C. H. HSIEH, AND R. A. HUGGINS, *J. Appl. Phys.* **46**, 2873 (1975).
12. C. TUBANDT, H. REINHOLD, AND G. LEIBOLD, *Z. Anorg. Allg. Chem.* **197**, 225 (1931).
13. F. BÉNIÈRE, *in* "Physics of Electrolytes," p. 299 (J. Hladik, Ed.), Academic Press (1972).
14. F. BÉNIÈRE, M. BÉNIÈRE, AND M. CHEMLA, *J. Phys. Chem. Solids* **31**, 1205 (1970).
15. T. G. STOEBE AND R. A. HUGGINS, *J. Mater. Sci.* **1**, 117 (1966).
16. V. Y. ANOSOV AND N. N. PATSUKOVA, *Russ. J. Inorg. Chem.* **1**, 104 (1956).
17. H. H. G. JELLINEK, *Trans. Faraday Soc.* **40**, 1 (1944).
18. "Gmelin Handbuch der Anorganische Chemie," p. 307. Blei Teil C. Lieferung 1, Verlag Chemie, Weinheim (1969).